

Ch. Zeoli · R. Machleidt · D. R. Entem

Infinite-cutoff renormalization of the chiral nucleon-nucleon interaction up to $N^3\text{LO}$

Dedicated to Professor Henryk Witala on the occasion of his 60th birthday.

Received: date / Accepted: date

Abstract Naively, the “best” method of renormalization is the one where a momentum cutoff is taken to infinity while maintaining stable results due to a cutoff-dependent adjustment of counterterms. We have applied this renormalization method in the non-perturbative calculation of phase-shifts for nucleon-nucleon (NN) scattering using chiral NN potentials up to next-to-next-to-next-to-leading order ($N^3\text{LO}$). For lower partial waves, we find that there is either no convergence with increasing order or, if convergence occurs, the results do not always converge to the empirical values. For higher partial waves, we always observe convergence to the empirical phase shifts (except for the $^3\text{G}_5$ state). Furthermore, no matter what the order is, one can use only one or no counterterm per partial wave, creating a rather erratic scheme of power counting that does not allow for a systematic order-by-order improvement of the predictions. The conclusion is that infinite-cutoff renormalization is inappropriate for chiral NN interactions, which should not come as a surprise, since the chiral effective field theory, these interactions are based upon, is designed for momenta below the chiral-symmetry breaking scale of about 1 GeV. Therefore, this value for the hard scale should also be perceived as the appropriate upper limit for the momentum cutoff.

Keywords Chiral perturbation theory · Nucleon-nucleon scattering · Non-perturbative renormalization

1 Introduction

During the past two decades, it has been demonstrated that chiral effective field theory (chiral EFT) represents a powerful tool to deal with hadronic interactions at low energy in a systematic and model-independent way (see Refs. [1; 2] for recent reviews). For the construction of an EFT, it is crucial to identify a separation of scales. In the hadron spectrum, a large gap between the masses of the pions and the masses of the vector mesons, like $\rho(770)$ and $\omega(782)$, can clearly be identified. Thus, it is natural to assume that the pion mass sets the soft scale, $Q \sim m_\pi$, and the rho mass the hard scale, $A_\chi \sim m_\rho \sim 1$ GeV, also known as the chiral-symmetry breaking scale. This is suggestive of considering

Ch. Zeoli
Department of Physics, University of Idaho, Moscow, Idaho 83844-0903, USA
Present address: Department of Physics, Florida State University, Tallahassee, Florida 32306-4350, USA
E-mail: cpz11@my.fsu.edu

R. Machleidt
Department of Physics, University of Idaho, Moscow, Idaho 83844-0903, USA
E-mail: machleid@uidaho.edu

D. R. Entem
Grupo de Fisica Nuclear and IUFFyM, University of Salamanca, E-37008 Salamanca, Spain
E-mail: entem@usal.es

a low-energy expansion arranged in terms of the soft scale over the hard scale, $(Q/\Lambda_\chi)^\nu$, where Q is generic for an external momentum (nucleon three-momentum or pion four-momentum) or a pion mass. The appropriate degrees of freedom are, obviously, pions and nucleons, and not quarks and gluons. To make sure that this EFT is not just another phenomenology, it must have a firm link with QCD. The link is established by having the EFT observe all relevant symmetries of the underlying theory, in particular, the broken chiral symmetry of low-energy QCD [3].

The early applications of chiral perturbation theory (ChPT) focused on systems like $\pi\pi$ [4] and πN [5], where the Goldstone-boson character of the pion guarantees that a perturbative expansion exists. But the past 15 years have also seen great progress in applying ChPT to nuclear forces [1; 2; 6; 7; 8; 9; 10; 11; 12; 13; 14; 15; 16; 17; 18; 19; 20; 21; 22; 23]. The nucleon-nucleon (NN) system is characterized by large scattering lengths and bound states indicating the non-perturbative character of the problem. Weinberg [6; 7] therefore suggested to calculate the nuclear amplitude in two steps. In step one, the *nuclear potential*, \hat{V} , is defined as the sum of irreducible diagrams, which are evaluated *perturbatively* up to the given order. Then in step two, this potential is iterated to all order (i.e., summed up *non-perturbatively*) in the Schrödinger or Lippmann-Schwinger (LS) equation:

$$\hat{T}(\mathbf{p}', \mathbf{p}) = \hat{V}(\mathbf{p}', \mathbf{p}) + \int d^3p'' \hat{V}(\mathbf{p}', \mathbf{p}'') \frac{M_N}{p^2 - p''^2 + i\epsilon} \hat{T}(\mathbf{p}'', \mathbf{p}), \quad (1)$$

where \hat{T} denotes the NN T-matrix and M_N the nucleon mass.

In general, the integral in the LS equation is divergent and needs to be regularized. One way to do this is by multiplying \hat{V} with a regulator function

$$\hat{V}(\mathbf{p}', \mathbf{p}) \mapsto \hat{V}(\mathbf{p}', \mathbf{p}) e^{-(p'/\Lambda)^{2n}} e^{-(p/\Lambda)^{2n}}. \quad (2)$$

Typical choices for the cutoff parameter Λ that appears in the regulator are $\Lambda \approx 0.5 \text{ GeV} \ll \Lambda_\chi \approx 1 \text{ GeV}$.

It is pretty obvious that results for the T-matrix may depend sensitively on the regulator and its cutoff parameter. This is acceptable if one wishes to build models. For example, the meson models of the past [24; 25] always depended sensitively on the choices for the cutoff parameters which, in fact, were important for the fit of the NN data. However, the EFT approach wishes to be fundamental in nature and not just another model.

In field theories, divergent integrals are not uncommon and methods have been developed for how to deal with them. One regulates the integrals and then removes the dependence on the regularization parameters (scales, cutoffs) by renormalization. In the end, the theory and its predictions do not depend on cutoffs or renormalization scales. So-called renormalizable quantum field theories, like QED, have essentially one set of prescriptions that takes care of renormalization through all orders. In contrast, EFTs are renormalized order by order.

The renormalization of *perturbative* EFT calculations is not a problem. *The problem is non-perturbative renormalization.* This problem typically occurs in *nuclear* EFT because nuclear physics is characterized by bound states which are non-perturbative in nature. EFT power counting may be different for non-perturbative processes as compared to perturbative ones. Such difference may be caused by the infrared enhancement of the reducible diagrams generated in the LS equation.

Weinberg's implicit assumption [6; 7; 26] was that the counterterms introduced to renormalize the perturbatively calculated potential, based upon naive dimensional analysis ("Weinberg counting"), are also sufficient to renormalize the non-perturbative resummation of the potential in the LS equation. In 1996, Kaplan, Savage, and Wise (KSW) [27; 28; 29] pointed out that there are problems with the Weinberg scheme if the LS equation is renormalized by minimally-subtracted dimensional regularization. This criticism resulted in a flurry of publications on the renormalization of the non-perturbative NN problem [30; 31; 32; 33; 34; 35; 36; 37; 38; 39; 40; 41; 42; 43; 44; 45; 46; 47; 48; 49; 50; 51; 52; 53; 54]. The literature is too comprehensive to discuss all contributions. Let us just mention some of the work that has particular relevance for our present discussion.

If the potential \hat{V} consists of contact terms only (a.k.a. pion-less theory), then the non-perturbative summation Eq. (1) can be performed analytically and the power counting is explicit. However, when pion exchange is included, then Eq. (1) can be solved only numerically and the power counting is less transparent. Perturbative ladder diagrams of arbitrarily high order, where the rungs of the ladder represent a potential made up from irreducible pion exchange, suggest that an infinite number of

counterterms is needed to achieve cutoff independence for all the terms of increasing order generated by the iterations. For that reason, KSW [27; 28; 29] proposed to sum the leading-order contact interaction to all orders (analytically) and to add higher-order contacts and pion exchange perturbatively up to the given order. Unfortunately, it turned out that the order by order convergence of one-pion exchange (1PE) is poor in the 3S_1 - 3D_1 state [30; 31]. The failure was triggered by the $1/r^3$ singularity of the 1PE tensor force when iterated to second order. Therefore, KSW counting is no longer taken into consideration (see, however, [47]). A balanced discussion of possible solutions can be found in [34].

Some researchers decided to take a second look at Weinberg's original proposal. A systematic investigation of Weinberg counting in leading order (LO) has been conducted by Nogga, Timmermans, and van Kolck [36] in momentum space, and by Valderrama and Arriola at LO and higher orders in configuration space [35; 37; 39]. A comprehensive discussion of both approaches and their equivalence can be found in [42; 48].

The LO NN potential consists of 1PE plus two nonderivative contact terms that contribute only in S waves. Nogga *et al* find that the given counterterms renormalize the S waves (i.e., stable results are obtained for $\Lambda \rightarrow \infty$) and the naively expected infinite number of counterterms is not needed. This means that Weinberg power counting does actually work in S waves at LO (ignoring the m_π dependence of the contact interaction discussed in Refs. [27; 28; 29; 34]). However, there are problems with a particular class of higher partial waves, namely those in which the tensor force from 1PE is attractive. The first few cases of this kind of low angular momentum are 3P_0 , 3P_2 , and 3D_2 , which need a counterterm for cutoff independence. The leading order (nonderivative) counterterms do not contribute in P and higher waves, which is why Weinberg counting fails in these cases. But the second order contact potential provides counterterms for P waves. Therefore, the promotion of, particularly, the 3P_0 and 3P_2 contacts from next-to-leading order (NLO) to LO would fix the problem in P waves. To take care of the 3D_2 problem, a next-to-next-to-next-to-leading order (N³LO) contact needs to be promoted to LO. Partial waves with orbital angular momentum $L \geq 3$ may be calculated in Born approximation with sufficient accuracy and, therefore, do not pose renormalization problems. In this way, one arrives at a scheme of ‘modified Weinberg counting’ [36] for the leading order two-nucleon interaction.

For a quantitative chiral NN potential one needs to advance all the way to N³LO [20]. Thus, the renormalization issue needs to be discussed beyond LO. Naively, the most perfect renormalization procedure is the one where the cutoff parameter Λ is carried to infinity while stable results are maintained. This was done successfully at LO in the work by Nogga *et al* [36] described above. At NNLO, the infinite-cutoff renormalization procedure has been investigated in [43; 44; 45] for partial waves with total angular momentum $J \leq 1$ and in [39] for all partial waves with $J \leq 5$. At N³LO, only a study of the 1S_0 state exists [42]. Thus, a full analysis of the issue is still lacking.

It is, therefore, the purpose of this paper to study the method of (non-perturbative) infinite-cutoff renormalization systematically order-by-order from LO to N³LO and for all partial-waves with $J \leq 6$. As discussed, it is necessary to carry this investigation through all of these orders, because the presently existing quantitative chiral NN potentials are of order N³LO and their renormalizability needs to be investigated.

This paper is organized as follows. In Sec. 2, we will present the chiral NN potential up to order N³LO and, in Sec. 3, the non-perturbative renormalization will be discussed. The order by order convergence (or non-convergence) is the subject of Sec. 4, and Sec. 5 will conclude the paper.

2 The chiral NN potential up to N³LO

EFTs are defined in terms of effective Lagrangians which are given by an infinite series of terms with increasing number of derivatives and/or nucleon fields, with the dependence of each term on the pion field prescribed by the rules of broken chiral symmetry. Applying this Lagrangian to a particular process, an unlimited number of Feynman graphs can be generated. Therefore, we need a scheme that makes the theory manageable and calculable. This scheme which tells us how to distinguish between large (important) and small (unimportant) contributions is ChPT, and determining the power ν of the expansion has become known as power counting.

Nuclear potentials are defined as sets of irreducible graphs up to a given order. The power ν of a few-nucleon diagram involving A nucleons is given in terms of naive dimensional analysis by:

$$\nu = -2 + 2A - 2C + 2L + \sum_i \Delta_i, \quad (3)$$

with

$$\Delta_i \equiv d_i + \frac{n_i}{2} - 2, \quad (4)$$

where C denotes the number of separately connected pieces and L the number of loops in the diagram; d_i is the number of derivatives or pion-mass insertions and n_i the number of nucleon fields (nucleon legs) involved in vertex i ; the sum runs over all vertices contained in the diagram under consideration. Note that $\Delta_i \geq 0$ for all interactions allowed by chiral symmetry. For an irreducible NN diagram (“two-nucleon potential”, $A = 2$, $C = 1$), Eq. (3) collapses to

$$\nu = 2L + \sum_i \Delta_i. \quad (5)$$

Thus, in terms of naive dimensional analysis or “Weinberg counting”, the various orders of the irreducible graphs which define the chiral NN potential are given by:

$$V_{\text{LO}} = V_{\text{ct}}^{(0)} + V_{1\pi}^{(0)} \quad (6)$$

$$V_{\text{NLO}} = V_{\text{LO}} + V_{\text{ct}}^{(2)} + V_{1\pi}^{(2)} + V_{2\pi}^{(2)} \quad (7)$$

$$V_{\text{NNLO}} = V_{\text{NLO}} + V_{1\pi}^{(3)} + V_{2\pi}^{(3)} \quad (8)$$

$$V_{\text{N}^3\text{LO}} = V_{\text{NNLO}} + V_{\text{ct}}^{(4)} + V_{1\pi}^{(4)} + V_{2\pi}^{(4)} + V_{3\pi}^{(4)} \quad (9)$$

where the superscript denotes the order ν of the low-momentum expansion. LO stands for leading order, NLO for next-to-leading order, etc.. Contact potentials carry the subscript “ct” and pion-exchange potentials can be identified by an obvious subscript.

The charge-independent 1PE potential reads

$$V_{1\pi}(\mathbf{p}', \mathbf{p}) = -\frac{g_A^2}{4f_\pi^2} \boldsymbol{\tau}_1 \cdot \boldsymbol{\tau}_2 \frac{\boldsymbol{\sigma}_1 \cdot \mathbf{q} \boldsymbol{\sigma}_2 \cdot \mathbf{q}}{q^2 + m_\pi^2}, \quad (10)$$

where \mathbf{p}' and \mathbf{p} designate the final and initial nucleon momenta in the center-of-mass system (CMS) and $\mathbf{q} \equiv \mathbf{p}' - \mathbf{p}$ is the momentum transfer; $\boldsymbol{\sigma}_{1,2}$ and $\boldsymbol{\tau}_{1,2}$ are the spin and isospin operators of nucleon 1 and 2; g_A , f_π , and m_π denote axial-vector coupling constant, the pion decay constant, and the pion mass, respectively. We use $f_\pi = 92.4$ MeV and $g_A = 1.29$ throughout this work. Since higher order corrections contribute only to mass and coupling constant renormalizations and since, on shell, there are no relativistic corrections, the on-shell 1PE has the form Eq. (10) in all orders.

In this paper, we will specifically calculate neutron-proton (np) scattering and take the charge-dependence (isospin violation) of the 1PE into account. Thus, the 1PE potential that we actually apply reads

$$V_{1\pi}^{(np)}(\mathbf{p}', \mathbf{p}) = -V_{1\pi}(m_{\pi^0}) + (-1)^{T+1} 2 V_{1\pi}(m_{\pi^\pm}), \quad (11)$$

where T denotes the isospin of the two-nucleon system and

$$V_{1\pi}(m_\pi) \equiv -\frac{g_A^2}{4f_\pi^2} \frac{\boldsymbol{\sigma}_1 \cdot \mathbf{q} \boldsymbol{\sigma}_2 \cdot \mathbf{q}}{q^2 + m_\pi^2}. \quad (12)$$

We use $m_{\pi^0} = 134.9766$ MeV and $m_{\pi^\pm} = 139.5702$ MeV.

2.1 Leading order (LO)

The LO chiral NN potential consists of a contact part and an 1PE part, cf. Eq. (6). The 1PE part is given by Eq. (11) and the LO contacts are

$$V_{\text{ct}}^{(0)}(\mathbf{p}', \mathbf{p}) = C_S + C_T \boldsymbol{\sigma}_1 \cdot \boldsymbol{\sigma}_2, \quad (13)$$

and, in terms of partial waves,

$$\begin{aligned} V_{\text{ct}}^{(0)}(^1S_0) &= \tilde{C}_{1S_0} = 4\pi (C_S - 3C_T) \\ V_{\text{ct}}^{(0)}(^3S_1) &= \tilde{C}_{3S_1} = 4\pi (C_S + C_T), \end{aligned} \quad (14)$$

where $C_S, C_T, \tilde{C}_{1S_0}, \tilde{C}_{3S_1}$ are constants.

2.2 Next-to-leading order (NLO)

Multi-pion exchange starts at NLO and continues through all higher orders. It involves divergent loop integrals that need to be regularized. An elegant way to do this is dimensional regularization which (besides the main nonpolynomial result) typically generates polynomial terms with coefficients that are, in part, infinite or scale dependent [13]. One purpose of the contacts is to absorb all infinities and scale dependencies and make sure that the final result is finite and scale independent. This is the renormalization of the perturbatively calculated NN potential, which must be carefully distinguished from the non-perturbative renormalization to be discussed in Sec. 3. The perturbative renormalization of the NN potential is very similar to what is done in the ChPT calculations of $\pi\pi$ and πN scattering, namely, a renormalization order by order, which is the method of choice for any EFT.

For the NLO chiral NN potential, Eq. (7), we need to specify the second order contact part and the two-pion exchange (2PE) part. The NLO contact terms are given by [1]

$$\begin{aligned} V_{\text{ct}}^{(2)}(\mathbf{p}', \mathbf{p}) &= C_1 q^2 + C_2 k^2 \\ &\quad + (C_3 q^2 + C_4 k^2) \boldsymbol{\sigma}_1 \cdot \boldsymbol{\sigma}_2 \\ &\quad + C_5 (-i\mathbf{S} \cdot (\mathbf{q} \times \mathbf{k})) \\ &\quad + C_6 (\boldsymbol{\sigma}_1 \cdot \mathbf{q}) (\boldsymbol{\sigma}_2 \cdot \mathbf{q}) \\ &\quad + C_7 (\boldsymbol{\sigma}_1 \cdot \mathbf{k}) (\boldsymbol{\sigma}_2 \cdot \mathbf{k}), \end{aligned} \quad (15)$$

with the partial-wave decomposition

$$\begin{aligned} V_{\text{ct}}^{(2)}(^1S_0) &= C_{1S_0} (p^2 + p'^2) \\ V_{\text{ct}}^{(2)}(^3P_0) &= C_{3P_0} pp' \\ V_{\text{ct}}^{(2)}(^1P_1) &= C_{1P_1} pp' \\ V_{\text{ct}}^{(2)}(^3P_1) &= C_{3P_1} pp' \\ V_{\text{ct}}^{(2)}(^3S_1) &= C_{3S_1} (p^2 + p'^2) \\ V_{\text{ct}}^{(2)}(^3S_1 - ^3D_1) &= C_{3S_1 - ^3D_1} p^2 \\ V_{\text{ct}}^{(2)}(^3D_1 - ^3S_1) &= C_{3S_1 - ^3D_1} p'^2 \\ V_{\text{ct}}^{(2)}(^3P_2) &= C_{3P_2} pp'. \end{aligned} \quad (16)$$

To state the 2PE potentials, we introduce the following notation:

$$\begin{aligned} V_{2\pi}(\mathbf{p}', \mathbf{p}) &= V_C + \boldsymbol{\tau}_1 \cdot \boldsymbol{\tau}_2 W_C \\ &\quad + [V_S + \boldsymbol{\tau}_1 \cdot \boldsymbol{\tau}_2 W_S] \boldsymbol{\sigma}_1 \cdot \boldsymbol{\sigma}_2 \\ &\quad + [V_{LS} + \boldsymbol{\tau}_1 \cdot \boldsymbol{\tau}_2 W_{LS}] (-i\mathbf{S} \cdot (\mathbf{q} \times \mathbf{k})) \\ &\quad + [V_T + \boldsymbol{\tau}_1 \cdot \boldsymbol{\tau}_2 W_T] \boldsymbol{\sigma}_1 \cdot \mathbf{q} \boldsymbol{\sigma}_2 \cdot \mathbf{q} \\ &\quad + [V_{\sigma L} + \boldsymbol{\tau}_1 \cdot \boldsymbol{\tau}_2 W_{\sigma L}] \boldsymbol{\sigma}_1 \cdot (\mathbf{q} \times \mathbf{k}) \boldsymbol{\sigma}_2 \cdot (\mathbf{q} \times \mathbf{k}), \end{aligned} \quad (17)$$

where

$$\begin{aligned}\mathbf{k} &\equiv \frac{1}{2}(\mathbf{p}' + \mathbf{p}) \text{ is the average momentum, and} \\ \mathbf{S} &\equiv \frac{1}{2}(\boldsymbol{\sigma}_1 + \boldsymbol{\sigma}_2) \text{ the total spin.}\end{aligned}\tag{18}$$

Using the above notation, the NLO 2PE is simply given by [1; 13]

$$W_C^{(2)} = -\frac{L(q)}{384\pi^2 f_\pi^4} \left[4m_\pi^2(5g_A^4 - 4g_A^2 - 1) + q^2(23g_A^4 - 10g_A^2 - 1) + \frac{48g_A^4 m_\pi^4}{w^2} \right], \tag{19}$$

$$V_T^{(2)} = -\frac{1}{q^2} V_S^{(2)} = -\frac{3g_A^4 L(q)}{64\pi^2 f_\pi^4}, \tag{20}$$

where

$$L(q) \equiv \frac{w}{q} \ln \frac{w+q}{2m_\pi} \tag{21}$$

and

$$w \equiv \sqrt{4m_\pi^2 + q^2}. \tag{22}$$

2.3 Next-to-next-to-leading order (NNLO)

There are no new contacts at NNLO, cf. Eq. (8), and, thus, all we need is the third order 2PE potential, which is [using the notation introduced in Eq. (17)] [1; 13]

$$V_C^{(3)} = V_{C1}^{(3)} + V_{C2}^{(3)}, \tag{23}$$

$$W_C^{(3)} = W_{C1}^{(3)} + W_{C2}^{(3)}, \tag{24}$$

$$V_T^{(3)} = V_{T1}^{(3)} + V_{T2}^{(3)}, \tag{25}$$

$$W_T^{(3)} = W_{T1}^{(3)} + W_{T2}^{(3)}, \tag{26}$$

$$V_S^{(3)} = V_{S1}^{(3)} + V_{S2}^{(3)}, \tag{27}$$

$$W_S^{(3)} = W_{S1}^{(3)} + W_{S2}^{(3)}, \tag{28}$$

$$V_{LS}^{(3)} = \frac{3g_A^4 \tilde{w}^2 A(q)}{32\pi M_N f_\pi^4}, \tag{29}$$

$$W_{LS}^{(3)} = \frac{g_A^2(1 - g_A^2)}{32\pi M_N f_\pi^4} w^2 A(q), \tag{30}$$

where

$$V_{C1}^{(3)} = \frac{3g_A^2}{16\pi f_\pi^4} \left\{ \frac{g_A^2 m_\pi^5}{16M_N w^2} - \left[2m_\pi^2(2c_1 - c_3) - q^2 \left(c_3 + \frac{3g_A^2}{16M_N} \right) \right] \tilde{w}^2 A(q) \right\}, \tag{31}$$

$$W_{C1}^{(3)} = \frac{g_A^2}{128\pi M_N f_\pi^4} \{ 3g_A^2 m_\pi^5 w^{-2} - [4m_\pi^2 + 2q^2 - g_A^2(4m_\pi^2 + 3q^2)] \tilde{w}^2 A(q) \}, \tag{32}$$

$$V_{T1}^{(3)} = -\frac{1}{q^2} V_{S1}^{(3)} = \frac{9g_A^4 \tilde{w}^2 A(q)}{512\pi M_N f_\pi^4}, \tag{33}$$

$$W_{T1}^{(3)} = -\frac{1}{q^2} W_{S1}^{(3)} = -\frac{g_A^2 A(q)}{32\pi f_\pi^4} \left[\left(c_4 + \frac{1}{4M_N} \right) w^2 - \frac{g_A^2}{8M_N} (10m_\pi^2 + 3q^2) \right], \tag{34}$$

and

$$V_{C2}^{(3)} = -\frac{3g_A^4}{256\pi f_\pi^4 M_N} (m_\pi w^2 + \tilde{w}^4 A(q)), \tag{35}$$

$$W_{C2}^{(3)} = \frac{g_A^4}{128\pi f_\pi^4 M_N} (m_\pi w^2 + \tilde{w}^4 A(q)), \tag{36}$$

$$V_{T2}^{(3)} = -\frac{1}{q^2} V_{S2}^{(3)} = \frac{3g_A^4}{512\pi f_\pi^4 M_N} (m_\pi + w^2 A(q)), \tag{37}$$

$$W_{T2}^{(3)} = -\frac{1}{q^2} W_{S2}^{(3)} = -\frac{g_A^4}{256\pi f_\pi^4 M_N} (m_\pi + w^2 A(q)), \tag{38}$$

with

$$A(q) \equiv \frac{1}{2q} \arctan \frac{q}{2m_\pi} \quad (39)$$

and

$$\tilde{w} \equiv \sqrt{2m_\pi^2 + q^2}. \quad (40)$$

Equations (35)-(38) are corrections of the iterative 2PE, see Ref. [1] for details. In all 2PE potentials, we use the average nucleon mass, $M_N = 938.9182$ MeV, and the average pion mass, $m_\pi = 138.039$ MeV. The values for the low-energy constants are $c_1 = -0.81$ GeV⁻¹, $c_3 = -3.20$ GeV⁻¹, and $c_4 = 5.40$ GeV⁻¹ [1].

2.4 Next-to-next-to-next-to-leading order (N³LO)

At N³LO, 14 new contact terms appear [1],

$$\begin{aligned} V_{\text{ct}}^{(4)}(\mathbf{p}', \mathbf{p}) = & D_1 q^4 + D_2 k^4 + D_3 q^2 k^2 + D_4 (\mathbf{q} \times \mathbf{k})^2 \\ & + (D_5 q^4 + D_6 k^4 + D_7 q^2 k^2 + D_8 (\mathbf{q} \times \mathbf{k})^2) \boldsymbol{\sigma}_1 \cdot \boldsymbol{\sigma}_2 \\ & + (D_9 q^2 + D_{10} k^2) (-i\mathbf{S} \cdot (\mathbf{q} \times \mathbf{k})) \\ & + (D_{11} q^2 + D_{12} k^2) (\boldsymbol{\sigma}_1 \cdot \mathbf{q}) (\boldsymbol{\sigma}_2 \cdot \mathbf{q}) \\ & + (D_{13} q^2 + D_{14} k^2) (\boldsymbol{\sigma}_1 \cdot \mathbf{k}) (\boldsymbol{\sigma}_2 \cdot \mathbf{k}) \\ & + D_{15} (\boldsymbol{\sigma}_1 \cdot (\mathbf{q} \times \mathbf{k}) \boldsymbol{\sigma}_2 \cdot (\mathbf{q} \times \mathbf{k})), \end{aligned} \quad (41)$$

which contribute as follows to the partial-wave potentials,

$$\begin{aligned} V_{\text{ct}}^{(4)}(^1S_0) &= \widehat{D}_{1S_0}(p'^4 + p^4) + D_{1S_0}p'^2 p^2 \\ V_{\text{ct}}^{(4)}(^3P_0) &= D_{3P_0}(p'^3 p + p' p^3) \\ V_{\text{ct}}^{(4)}(^1P_1) &= D_{1P_1}(p'^3 p + p' p^3) \\ V_{\text{ct}}^{(4)}(^3P_1) &= D_{3P_1}(p'^3 p + p' p^3) \\ V_{\text{ct}}^{(4)}(^3S_1) &= \widehat{D}_{3S_1}(p'^4 + p^4) + D_{3S_1}p'^2 p^2 \\ V_{\text{ct}}^{(4)}(^3D_1) &= D_{3D_1}p'^2 p^2 \\ V_{\text{ct}}^{(4)}(^3S_1 - ^3D_1) &= \widehat{D}_{3S_1-3D_1}p^4 + D_{3S_1-3D_1}p'^2 p^2 \\ V_{\text{ct}}^{(4)}(^3D_1 - ^3S_1) &= \widehat{D}_{3S_1-3D_1}p'^4 + D_{3S_1-3D_1}p'^2 p^2 \\ V_{\text{ct}}^{(4)}(^1D_2) &= D_{1D_2}p'^2 p^2 \\ V_{\text{ct}}^{(4)}(^3D_2) &= D_{3D_2}p'^2 p^2 \\ V_{\text{ct}}^{(4)}(^3P_2) &= D_{3P_2}(p'^3 p + p' p^3) \\ V_{\text{ct}}^{(4)}(^3P_2 - ^3F_2) &= D_{3P_2-3F_2}p' p^3 \\ V_{\text{ct}}^{(4)}(^3F_2 - ^3P_2) &= D_{3P_2-3F_2}p'^3 p \\ V_{\text{ct}}^{(4)}(^3D_3) &= D_{3D_3}p'^2 p^2. \end{aligned} \quad (42)$$

The 2PE contributions at this order, $V_{2\pi}^{(4)}$, are very involved, which is why we will not reprint them here. The comprehensive expressions can be found in Appendix D of Ref. [1]. We note that, in the calculations of this paper, we apply *all* N³LO 2PE terms including those which require numerical integrations. The parameters we use in this work are listed in column “NN potential” of Table 2 of Ref. [1].

The N³LO three-pion exchange (3PE) contributions $V_{3\pi}^{(4)}$, cf. Eq. (9), are left out, since they have been found to be negligible [55; 56].

3 NN scattering and non-perturbative renormalization

For the unitarizing scattering equation, we choose the relativistic three-dimensional equation proposed by Blankenbecler and Sugar (BbS) [57], which reads,

$$T(\mathbf{p}', \mathbf{p}) = V(\mathbf{p}', \mathbf{p}) + \int \frac{d^3 p''}{(2\pi)^3} V(\mathbf{p}', \mathbf{p}'') \frac{M_N^2}{E_{p''}} \frac{1}{p^2 - p''^2 + i\epsilon} T(\mathbf{p}'', \mathbf{p}) \quad (43)$$

with $E_{p''} \equiv \sqrt{M_N^2 + p''^2}$. The advantage of using a relativistic scattering equation is that it automatically includes relativistic corrections to all orders. Thus, in the scattering equation, no propagator modifications are necessary when raising the order to which the calculation is conducted.

Defining

$$\hat{V}(\mathbf{p}', \mathbf{p}) \equiv \frac{1}{(2\pi)^3} \sqrt{\frac{M_N}{E_{p'}}} V(\mathbf{p}', \mathbf{p}) \sqrt{\frac{M_N}{E_p}} \quad (44)$$

and

$$\hat{T}(\mathbf{p}', \mathbf{p}) \equiv \frac{1}{(2\pi)^3} \sqrt{\frac{M_N}{E_{p'}}} T(\mathbf{p}', \mathbf{p}) \sqrt{\frac{M_N}{E_p}}, \quad (45)$$

where the factor $1/(2\pi)^3$ is added for convenience, the BbS equation collapses into the usual, nonrelativistic Lippmann-Schwinger (LS) equation, Eq. (1). Since \hat{V} satisfies Eq. (1), it can be used like a usual nonrelativistic potential, and \hat{T} may be perceived as the conventional nonrelativistic T-matrix. The square-root factors in Eqs. (44) and (45) are applied to the potentials of all orders except in LO.

In the LS equation, Eq. (1), we use

$$M_N = \frac{2M_p M_n}{M_p + M_n} = 938.9182 \text{ MeV}, \text{ and} \quad (46)$$

$$p^2 = \frac{M_p^2 T_{\text{lab}} (T_{\text{lab}} + 2M_n)}{(M_p + M_n)^2 + 2T_{\text{lab}} M_p}, \quad (47)$$

where $M_p = 938.2720$ MeV and $M_n = 939.5653$ MeV are the proton and neutron masses, respectively, and T_{lab} is the kinetic energy of the incident neutron in the laboratory system (“Lab. Energy”). The relationship between p^2 and T_{lab} is based upon relativistic kinematics.

We renormalize the LO chiral NN potential as described in Refs. [36; 49] and discussed in the Introduction. We then perform the infinite-cutoff renormalization also for the NLO, NNLO, and $N^3\text{LO}$ chiral NN potentials. This is accomplished by studying the dependence of the phase shifts on the cutoff parameter Λ that appears in the regulator function, Eq. (2). We vary Λ over a wide range, from 0.5 GeV to 10 GeV (with $n = 2$ for the LO, NLO, and NNLO potentials, and $n = 3$ for $N^3\text{LO}$).

For partial-waves with short-range repulsion, convergence with increasing cutoff values is obtained without the use of any counterterm, i.e., convergence occurs “automatically”. In fact, in these cases, any counterterm becomes ineffective for large cutoffs. Thus, no counterterm is used in partial-waves with short-range repulsion.

For partial-waves with short-range attraction, one counterterm (contact term) is needed to ensure convergence. If we introduce a second counterterm per partial-wave, it turns out that this second parameter becomes ineffective for large cutoffs. Thus, we apply only one counterterm, which we use to fit the following empirical information. In S -waves, we fit the scattering lengths; $^1S_0 : a_s = -23.740$ fm, $^3S_1 : a_t = 5.417$ fm. In the other partial-waves with $J \leq 2$, we fit the phase shift at $T_{\text{lab}} = 50$ MeV to the central value from the Nijmegen multi-energy np phase-shift analysis [58]. For $J \geq 3$, we fit the phase-shift at 100 MeV or 200 MeV.

In summary, at any order, either one or no counterterm is needed in each partial-wave for the infinite-cutoff renormalization. We show this in the left half of Table 1 for the various partial-wave states. The right half of Table 1 shows the number of counterterms according to Weinberg Counting. Obviously, there are large differences between the two schemes. The higher partial-wave states that are not listed in the table do not receive counterterms.

Table 1 Number of counterterms per partial-wave as required in two different renormalization schemes.

Partial-Wave	Infinite-cutoff renormalization				Weinberg Counting		
	LO	NLO	NNLO	N ³ LO	LO	NLO/NNLO	N ³ LO
¹ S ₀	1	1	1	1	1	2	4
³ P ₀	1	0	0	0	0	1	2
¹ P ₁	0	0	0	0	0	1	2
³ P ₁	0	1	1	1	0	1	2
³ S ₁	1	0	1	1	1	2	4
³ S ₁ - ³ D ₁	0	0	1	0	0	1	3
³ D ₁	0	0	0	0	0	0	1
¹ D ₂	0	1	1	1	0	0	1
³ D ₂	1	0	1	0	0	0	1
³ P ₂	1	1	1	1	0	1	2
³ P ₂ - ³ F ₂	0	0	0	0	0	0	1
³ F ₂	0	0	0	0	0	0	0
¹ F ₃	0	0	0	0	0	0	0
³ F ₃	0	0	1	1	0	0	0
³ D ₃	0	0	1	0	0	0	1
³ D ₃ - ³ G ₃	0	0	0	0	0	0	0
³ G ₃	0	0	0	0	0	0	0
¹ G ₄	0	0	1	1	0	0	0
³ G ₄	0	0	0	0	0	0	0
³ F ₄	0	0	1	1	0	0	0

We have obtained convergence with increasing cutoff for all phase parameters with $J \leq 6$ in each order, NLO, NNLO, and N³LO. As evident from Table 1, in NNLO and N³LO, we need counterterms (contact terms) for the renormalization of the ³F₃, ³F₄, and ¹G₄ waves. These terms are:

$$V_{ct}^{(6)}(^3F_3) = E_{^3F_3} p'^3 p^3, \quad (48)$$

$$V_{ct}^{(6)}(^3F_4) = E_{^3F_4} p'^3 p^3, \quad (49)$$

$$V_{ct}^{(8)}(^1G_4) = F_{^1G_4} p'^4 p^4. \quad (50)$$

In Figures 1 and 2, we demonstrate the convergence of the phase parameters with increasing cutoff for the N³LO potential in partial-wave with $J \leq 2$. The black dotted curve is obtained for $\Lambda = 0.5$ GeV, the blue dashed curve for $\Lambda = 1$ GeV, the green dash-dot curve for $\Lambda = 5$ GeV, and the red solid curve for $\Lambda = 10$ GeV. The fact that the green and red curves are essentially indistinguishable in those figures, demonstrates that convergence for large cutoffs has occurred. However, it is also clearly seen in these figures that, even though we are here at a relatively high order (N³LO), the cutoff-converged curves show large discrepancies with respect to the empirical phase shifts in several partial waves, particularly, ¹S₀, ³S₁, ³D₁, ³D₂, and ϵ_2 . This issue will be further discussed in the next section.

4 Order By Order Convergence

Having accomplished the infinite-cutoff renormalization of the four orders we consider, it is now of interest to investigate the order-by-order convergence of these cutoff-converged cases. This is done in Figs. 3-8.

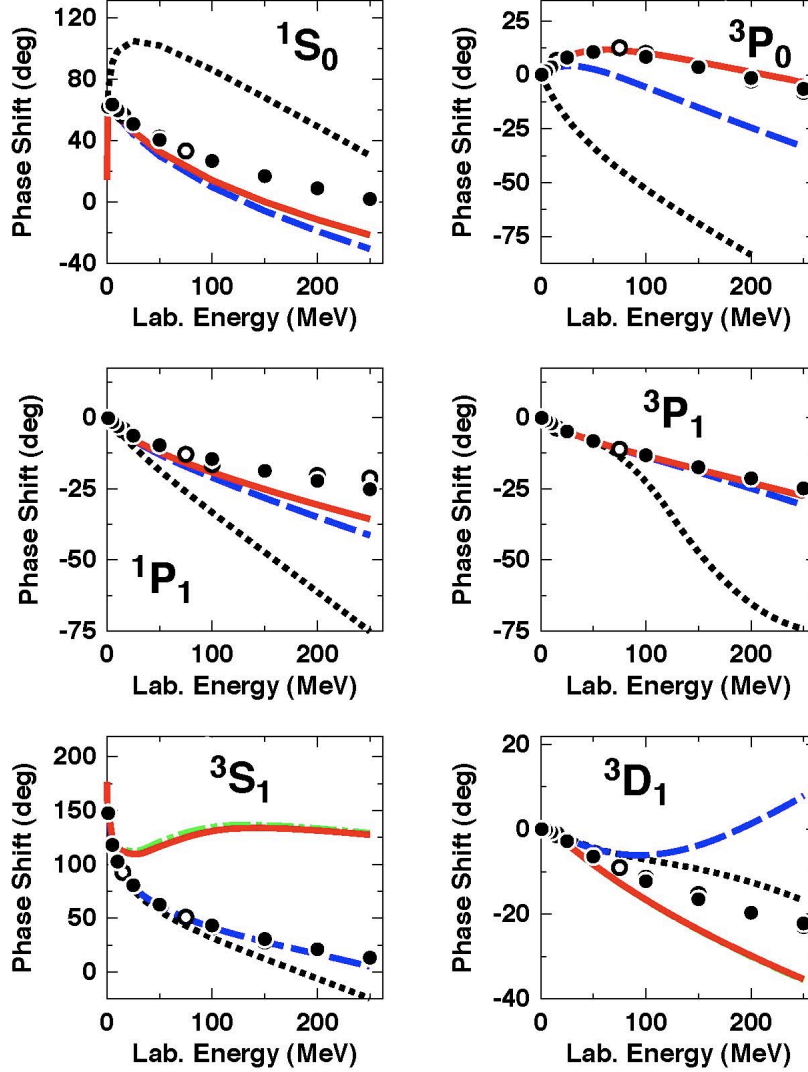


Fig. 1 Phase-shifts of neutron-proton scattering at order $N^3\text{LO}$ for total angular momentum $J \leq 1$ and laboratory kinetic energies below 250 MeV. The black dotted curve is obtained for $\Lambda = 0.5$ GeV, the blue dashed curve for $\Lambda = 1$ GeV, the green dash-dot curve for $\Lambda = 5$ GeV, and the red solid curve for $\Lambda = 10$ GeV. Note that the curves for $\Lambda = 5$ GeV and 10 GeV are, in general, indistinguishable on the scale of the figure. The filled and open circles represent the results from the Nijmegen multi-energy np phase-shift analysis [58] and the VPI/GWU single-energy np analysis SM99 [59], respectively.

In Fig. 3, the $S = 0$, $T = 1$ np phase-shifts for $L \leq 6$ are displayed, where S denotes the total spin, T the total isospin, and L the orbital angular momentum of the two-nucleon system. Note that, in each order, the underlying analytic expression for the potential is the same except that it is decomposed into partial-waves with $L = 0, 2, 4$, and 6. The effect of this partial-wave decomposition is that the short-range part of the two-nucleon potential is increasingly suppressed with growing L ; or in other words, the “centrifugal barrier” becomes larger with L . In the 1S_0 state, the phase-shifts are (almost) converged at $N^3\text{LO}$, but do not reproduce the empirical phase-shifts. This is consistent with what was found in Ref. [42]. However, at the next higher $S = 0$, $T = 1$ partial-wave, the 1D_2 , we observe that the phase-shift prediction converges to the empirical phase-shift values, and this is also true for all higher $S = 0$, $T = 1$ partial-waves shown in Fig. 3.

In Fig. 4, we show the $S = 0$, $T = 0$ state for various partial-waves up to $L = 5$. The situation is very similar to what we just discussed. In the lowest partial-wave, the 1P_1 , we have (almost) convergence,

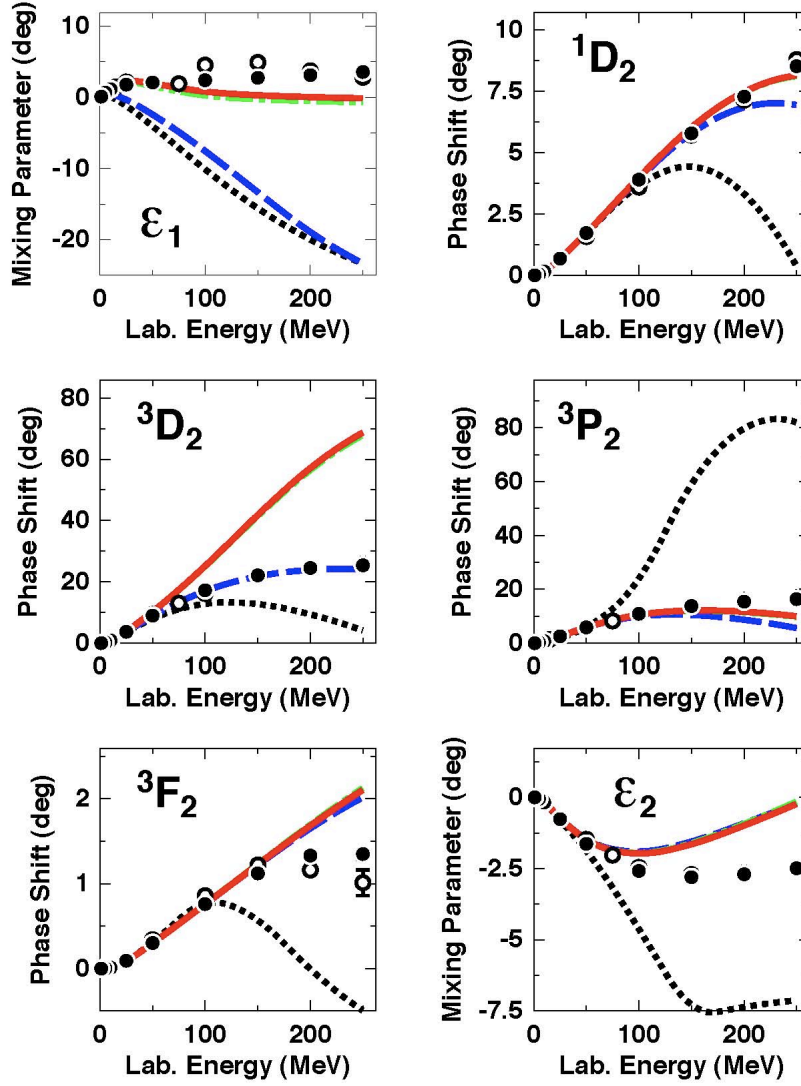


Fig. 2 Same as Fig. 1, but $J = 2$ phase-shifts and $J \leq 2$ mixing parameters are shown

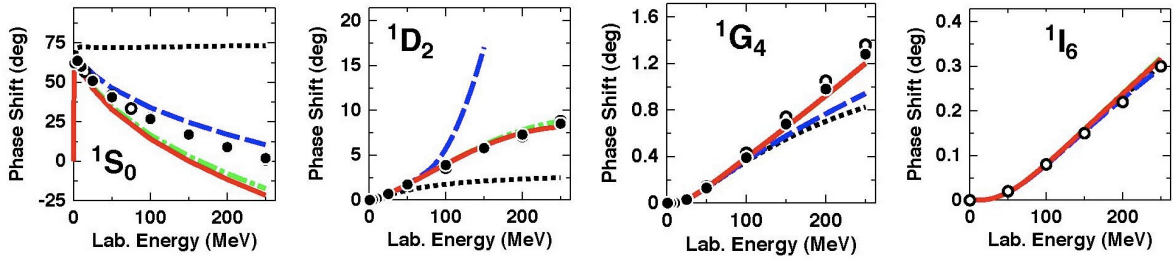


Fig. 3 Renormalized np phase-shifts at order LO (black dotted curve), NLO (blue dashed curve), NNLO (green dash-dotted curve), and $N^3\text{LO}$ (red solid curve). The $S = 0$, $T = 1$ phase shifts with $L \leq 6$ are shown for energies below 250 MeV. Filled and open circles are as described in Fig. 1.

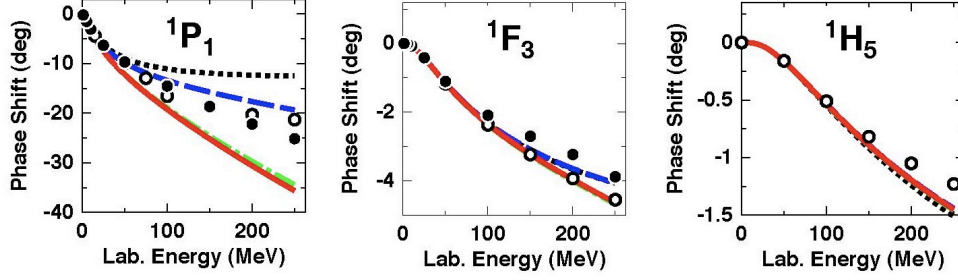


Fig. 4 Renormalized $S = 0$, $T = 0$ np phase-shifts with $L \leq 5$. Notation as in Fig. 3.

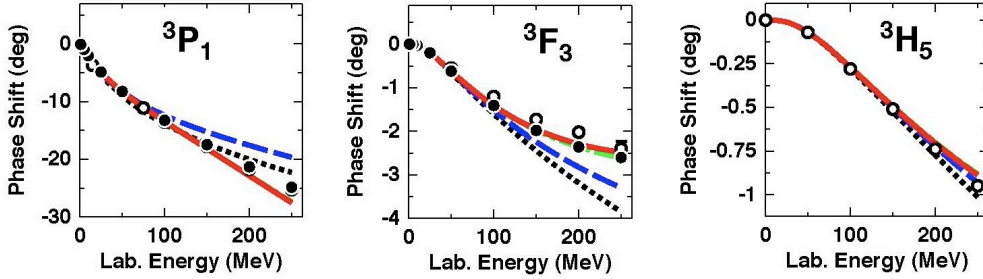


Fig. 5 Renormalized $S = 1$, $T = 1$ uncoupled np phase-shifts with $L \leq 5$. Notation as in Fig. 3.

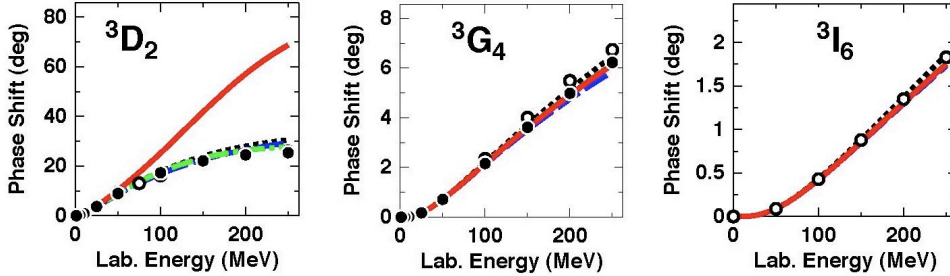


Fig. 6 Renormalized $S = 1$, $T = 0$ uncoupled np phase-shifts for $L \leq 6$. Notation as in Fig. 3.

though not to the empirical values. In higher partial-waves, however, the predictions converge to the experimental phase-shifts. This finishes the discussion of (spin) singlet states ($S = 0$).

Now we turn to (spin) triplet states ($S = 1$). Here, we need to distinguish between uncoupled and coupled partial-waves and will discuss the former first. The phase-shift predictions for uncoupled $S = 1$, $T = 1$ states are shown in Fig. 5 and for $S = 1$, $T = 0$ in Fig. 6. Good convergence to the empirical phase-shifts is observed for all $S = 1$, $T = 1$ partial-waves (including the lowest one, 3P_1). In contrast, for $S = 1$, $T = 0$, a strong divergence occurs at N³LO in the 3D_2 state (first frame of Fig. 6), while the higher $S = 1$, $T = 0$ partial-waves converge well.

Finally, we discuss the coupled cases. The $T = 1$ coupled partial-waves are displayed in Fig. 7. We include here the 3P_0 state, such that we can compare it with its counterparts of larger L , namely 3F_2 , 3H_4 , and 3K_6 . It is clearly seen that the 3P_0 shows no order-by-order convergence, while the 3F_2 has near convergence and the 3H_4 and 3K_6 states are fully converged to the empirical information. The associated coupled partial-waves show corresponding trends.

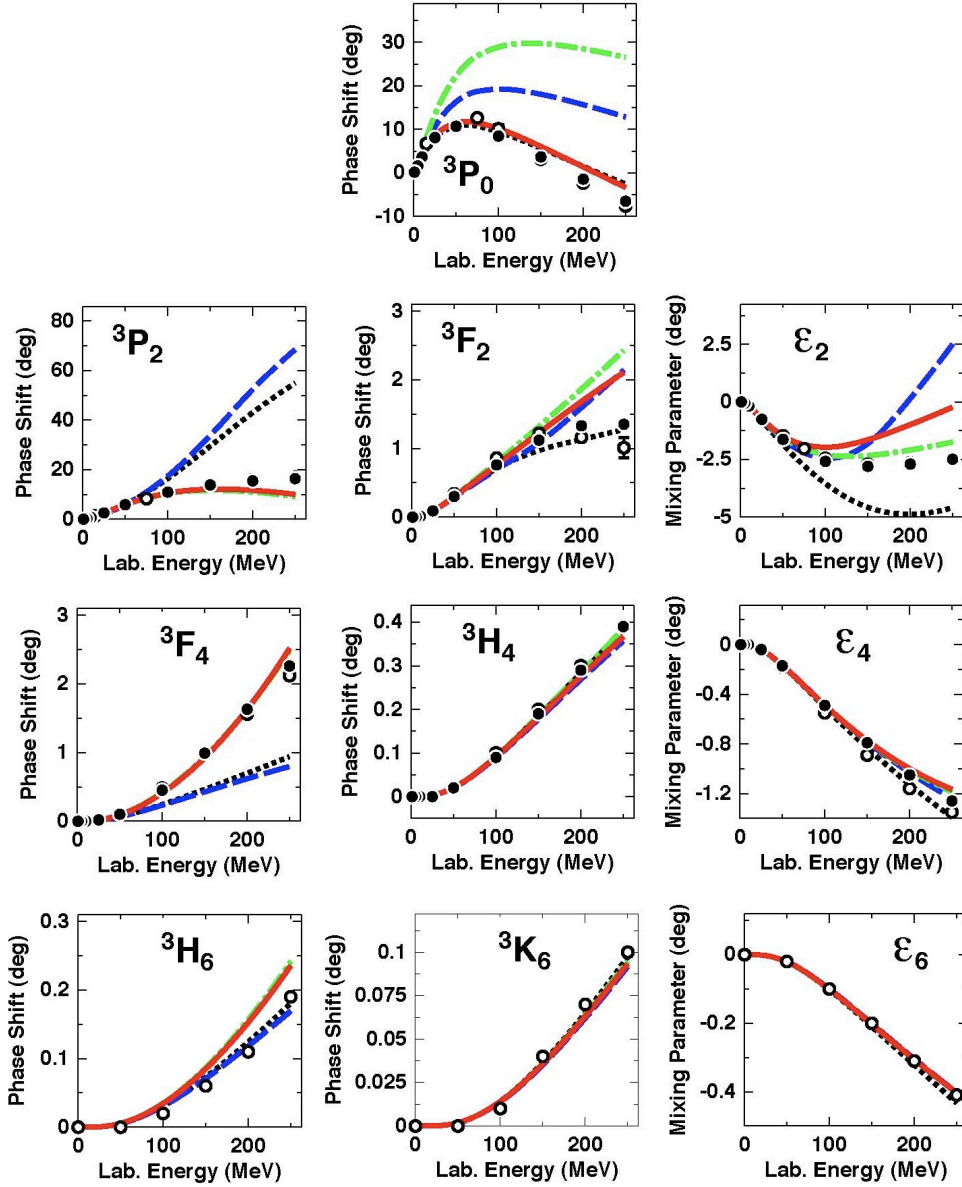


Fig. 7 The renormalized 3P_0 and renormalized $S = 1, T = 1$ coupled np phase parameters for $J \leq 6$. Notation as in Fig. 3.

The last set of partial-waves to be discussed are the $S = 1, T = 0$ coupled states shown in Fig. 8. While there is no convergence with increasing orders for the $J = 1$ states, converged results and agreement with the experimental parameters are seen in the $L = J + 1$ partial-waves (3G_3 and 3I_5) and in the mixing parameters with $J \geq 3$ (i.e., ε_3 and ε_5). Contrary to this, the $L = J - 1$ waves (${}^3S_1, {}^3D_3, {}^3G_5$) never converge. Even in the rather high partial-wave, 3G_5 , there is a large difference between the NNLO and N^3 LO predictions. This phenomenon may be related to the fact that the 3G_5 is the only higher partial-wave that disagrees with the empirical phase-shifts at N^3 LO, as was noticed already in Ref. [19]. At the present time, we do not have an explanation for this problem.

The observations we have made in conjunction with Figs. 3-8 can be summarized as follows: Some lower partial-waves show no convergence and no order-by-order improvement. On the other hand, all higher partial-waves (except for the notorious 3G_5) do not only converge, they also converge to the empirical values. Note that in higher partial-waves the short-range part of the NN interaction

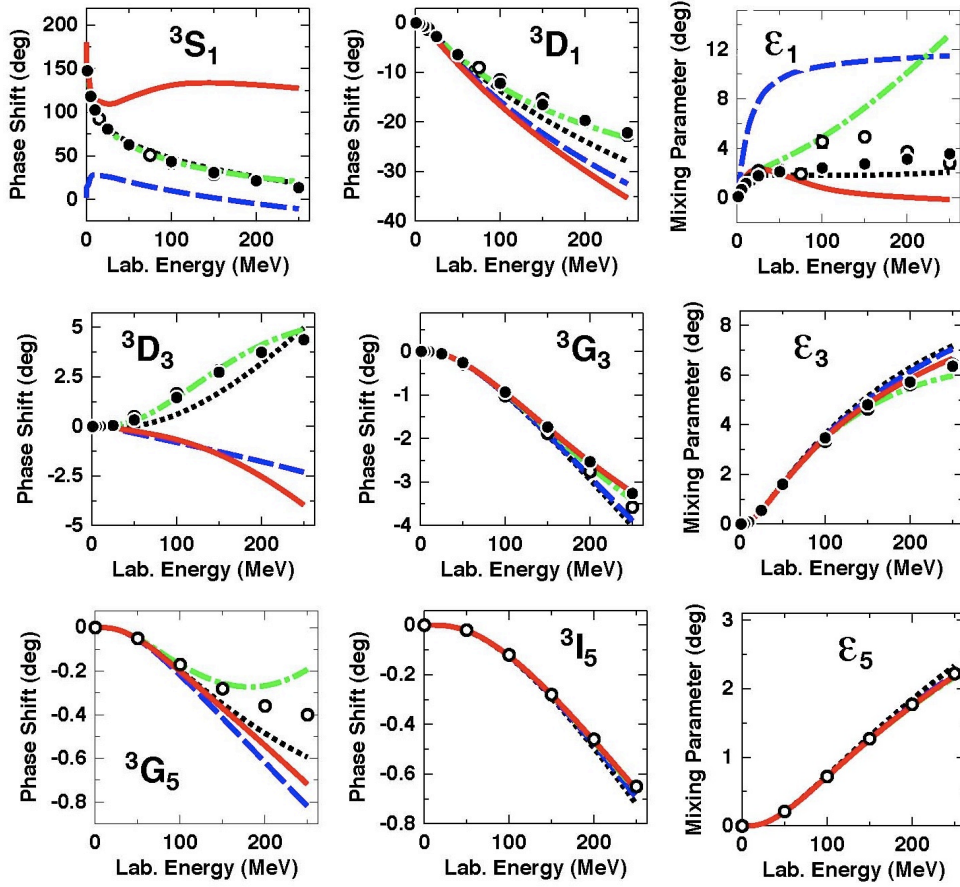


Fig. 8 Renormalized $S = 1$, $T = 0$ coupled np phase parameters for $J \leq 5$. Notation as in Fig. 3.

(equivalent to the high-momentum components of the interaction) is suppressed by the centrifugal barrier. This suggests that the long- and intermediate-range part of the NN potential up to $N^3\text{LO}$ is reasonable, while the short-range part may be, in part, un-physical.

In the infinite-cutoff renormalization the potential is admitted up to unlimited momenta. However, the EFT this potential is derived from has validity only for momenta smaller than the chiral symmetry breaking scale $\Lambda_\chi \approx 1$ GeV. The lack of order-by-order convergence and the discrepancies in lower partial-waves demonstrate that the potential should not be used beyond the limits of the effective theory (see Ref. [60] for a related discussion). The conclusion then is that cutoffs should be limited to $\Lambda \lesssim \Lambda_\chi$.

5 Summary and Conclusions

We have investigated a particular scheme for the non-perturbative renormalization of the nucleon-nucleon (NN) potential based upon chiral effective field theory (chiral EFT). In the scheme applied, the cutoff parameter of the regulator is taken to infinity.

Two vital requirements for constituting the legitimacy of an EFT are regulator independence and a power counting scheme that allows for order-by-order improvements of the predictions. We were able to achieve regulator independence (i.e., cutoff-independence) for all orders of chiral perturbation theory considered (i.e., LO, NLO, NNLO, and $N^3\text{LO}$) and all partial-waves up to $J = 6$. In general, cutoff-independence is seen for cutoff values above 5 GeV.

However, in this investigation, we have also observed that large cutoffs impose limitations on the effectiveness of counterterms. In each partial-wave, either no counterterm (case of short-range repulsion)

or one counterterm (case of short-range attraction) is effective. Therefore, the power counting scheme implied by the infinite-cutoff method is considerably different from the one of Naive Dimensional Analysis or Weinberg Counting (cf. Table 1). As a consequence, order-by-order improvements of the predictions do not occur in several lower partial-waves.

Thus, the chiral EFT approach to nuclear forces fails when renormalized by the infinite-cutoff method. This result may not come as a surprise considering that the EFT which we apply is designed for momenta below the chiral-symmetry breaking scale, $\Lambda_\chi \approx 1$ GeV. Under the infinite-cutoff method, the potential contributes for momenta that are far beyond the hard scale of 1 GeV. Our results suggest that finite-cutoffs $\lesssim 1$ GeV should be used for the non-perturbative regularization of the chiral NN potential. With such cutoffs, all counterterms of Weinberg Counting are effective, and an order-by-order improvement of the predictions is to be expected [61].

Acknowledgements The authors gratefully acknowledge enlightening discussions with E. Ruiz Arriola and M. Pavon Valderrama. The work by R. M. was supported in part by the U.S. Department of Energy under Grant No. DE-FG02-03ER41270. The work of D. R. E. was funded by the Ministerio de Ciencia y Tecnología under Contract No. FPA2007-65748, the Junta de Castilla y León under Contract No. GR12, and the European Community-Research Infrastructure Integrating Activity “Study of Strongly Interacting Matter” (HadronPhysics2 Grant No. 227431).

References

1. Machleidt R., Entem D.R.: Chiral effective field theory and nuclear forces. *Phys. Rep.* **503**, 1 (2011)
2. Epelbaum, E., Hammer, H.-W., Meißner, U.-G.: Modern theory of nuclear forces. *Rev. Mod. Phys.* **81**, 1773 (2009)
3. Weinberg S.: Phenomenological Lagrangians. *Physica* **96A**, 327 (1979)
4. Gasser J., Leutwyler H.: Chiral Perturbation Theory to One Loop. *Ann. Phys. (N.Y.)* **158**, 142 (1984)
5. Gasser J., Sainio M.E., Švarc A.: Nucleons with Chiral Loops. *Nucl. Phys.* **B307**, 779 (1988)
6. Weinberg S.: Nuclear forces from chiral lagrangians. *Phys. Lett. B* **251**, 288 (1990)
7. Weinberg S.: Effective Chiral Lagrangians for Nucleon-Pion Interactions and Nuclear Forces. *Nucl. Phys.* **B363**, 3 (1991)
8. Weinberg S.: Three-body interactions among nucleons and pions. *Phys. Lett. B* **295**, 114 (1992)
9. Ordóñez C., Ray L., van Kolck U.: Nucleon-Nucleon Potential from an Effective Chiral Lagrangian. *Phys. Rev. Lett.* **72**, 1982 (1994)
10. Ordóñez C., Ray L., van Kolck U.: Two-nucleon potential from chiral Lagrangians. *Phys. Rev. C* **53**, 2086 (1996)
11. van Kolck U.: Few-nucleon forces from chiral Lagrangians. *Phys. Rev. C* **49**, 2932 (1994)
12. van Kolck U.: Effective Field Theory of Nuclear Forces. *Prog. Part. Nucl. Phys.* **43**, 337 (1999)
13. Kaiser N., Brockmann R., Weise W.: Peripheral nucleon-nucleon phase shifts and chiral symmetry. *Nucl. Phys.* **A625**, 758 (1997)
14. Kaiser N., Gerstendörfer S., Weise W.: Peripheral NN-scattering: role of delta-excitation, correlated two-pion and vector meson exchange. *Nucl. Phys.* **A637**, 395 (1998)
15. Epelbaum E., Glöckle W., Meißner U.-G.: Nuclear forces from chiral Lagrangians using the method of unitary transformations (I): Formalism. *Nucl. Phys.* **A637**, 107 (1998)
16. Epelbaum E., Glöckle W., Meißner U.-G.: Nuclear forces from chiral Lagrangians using the method of unitary transformations (II): The two-nucleon system. *Nucl. Phys.* **A671**, 295 (2000)
17. Bedaque P.F., van Kolck U.: Effective Field Theory for Few-Nucleon Systems. *Ann. Rev. Nucl. Part. Sci.* **52**, 339 (2002)
18. Entem D.R., Machleidt R.: Accurate nucleon-nucleon potential based upon chiral perturbation theory. *Phys. Lett. B* **524**, 93 (2002)
19. Entem D.R., Machleidt R.: Chiral 2π exchange at fourth order and peripheral NN scattering. *Phys. Rev. C* **66**, 014002 (2002)
20. Entem D.R., Machleidt R.: Accurate charge-dependent nucleon-nucleon potential at fourth order of chiral perturbation theory. *Phys. Rev. C* **68**, 041001(R) (2003)
21. Machleidt R., Entem D.R.: Towards a consistent approach to nuclear structure: EFT of two- and many-body forces. *J. Phys. G: Nucl. Part. Phys.* **31**, S1235 (2005)
22. Epelbaum E., Glöckle W., Meißner U.-G.: The two-nucleon system at next-to-next-to-next-to-leading order. *Nucl. Phys.* **A747**, 362 (2005)
23. Machleidt R., Entem D.R.: Nuclear forces from chiral EFT: the unfinished business. *J. Phys. G: Nucl. Part. Phys.* **37**, 064041 (2010)
24. Machleidt R.: The Meson Theory of Nuclear Forces and Nuclear Structure. *Adv. Nucl. Phys.* **19**, 189 (1989)
25. Machleidt R., Holinde K., Elster Ch.: The Bonn Meson-Exchange Model for The Nucleon-Nucleon Interaction. *Phys. Rep.* **149**, 1 (1987)
26. Weinberg S.: Effective Field Theory, Past and Future. arXiv:0908.1964 [hep-th]

27. Kaplan D.B., Savage M.J., Wise M.B.: Nucleon-Nucleon Scattering from Effective Field Theory. Nucl. Phys. **B478**, 629 (1996)
28. Kaplan D.B., Savage M.J., Wise M.B.: A New Expansion for Nucleon-Nucleon Interactions. Phys. Lett. B **424**, 390 (1998)
29. Kaplan D.B., Savage M.J., Wise M.B.: Two-nucleon system from effective field theory. Nucl. Phys. **B534**, 329 (1998)
30. Fleming, S., Mehen, T., Stewart, I.W.: NNLO corrections to nucleon-nucleon scattering and perturbative pions. Nucl. Phys. **A677**, 313 (2000)
31. Fleming, S., Mehen, T., Stewart, I.W.: The N N scattering 3S1 - 3D1 mixing angle at NNLO. Phys. Rev. C **61** (2000) 044005.
32. Phillips, D.R., Beane, S.R., Cohen, T.D.: Nonperturbative regularization and renormalization: Simple examples from nonrelativistic quantum mechanics. Ann. Phys. (N.Y.) **263**, 255 (1998)
33. Frederico, T., Timoteo, V.S., Tomio, L.: Renormalization of the one pion exchange interaction. Nucl. Phys. **A653**, 209 (1999)
34. Beane, S.R., Bedaque, P.F., Savage, M.J., van Kolck, U.: Towards a perturbative theory of nuclear forces. Nucl. Phys. **A700**, 377 (2002)
35. Pavon Valderrama, M., Ruiz Arriola, E.: Renormalization of the deuteron with one pion exchange. Phys. Rev. C **72**, 054002 (2005)
36. Nogga A., Timmermans R.G.E., van Kolck U.: Renormalization of one-pion exchange and power counting. Phys. Rev. C **72**, 054006 (2005)
37. Pavon Valderrama, M., Ruiz Arriola, E.: Renormalization of NN interaction with chiral two pion exchange potential. central phases and the deuteron. Phys. Rev. C **74**, 054001 (2006)
38. M. C. Birse, Phys. Rev. C **74** (2006) 014003; Phys. Rev. C **76** (2007) 034002.
39. Pavon Valderrama M., Ruiz Arriola E.: Renormalization of the NN interaction with a chiral two-pion exchange potential. II. Noncentral phases. Phys. Rev. C **74**, 064004 (2006); Erratum. Phys. Rev. C **75**, 059905 (2007)
40. Epelbaum, E., Meißner, U.-G.: On the renormalization of the one-pion exchange potential and the consistency of Weinberg's power counting. arXiv:nucl-th/0609037.
41. Pavon Valderrama M., Ruiz Arriola E.: Renormalization group analysis of boundary conditions in potential scattering. Ann. Phys. (N.Y.) **323**, 1037 (2008)
42. Entem D.R., Ruiz Arriola E., Pavón Valderrama M., Machleidt R.: Renormalization of chiral two-pion exchange NN interactions: Momentum space versus coordinate space. Phys. Rev. C **77**, 044006 (2008)
43. Yang C.-J., Elster Ch., Phillips D.R.: Subtractive renormalization of the NN scattering amplitude at leading order in chiral effective theory. Phys. Rev. C **77**, 014002 (2008)
44. Yang C.-J., Elster Ch., Phillips D.R.: Subtractive renormalization of the chiral potentials up to next-to-next-to-leading order in higher NN partial waves. Phys. Rev. C **80**, 034002 (2009)
45. Yang C.-J., Elster Ch., Phillips D.R.: Subtractive renormalization of the NN interaction in chiral effective theory up to next-to-next-to-leading order: S waves. Phys. Rev. C **80**, 044002 (2009)
46. Long B., van Kolck U.: Renormalization of singular potentials and power counting. Ann. Phys. (N.Y.) **323**, 1304 (2008)
47. Beane, S.R., Kaplan, D.B., Vuorinen, A.: Perturbative nuclear physics. Phys. Rev. C **80**, 011001 (2009)
48. Pavon Valderrama, M., Nogga, A., Ruiz Arriola, E., Phillips, D.R.: Deuteron form factors in chiral effective theory: Regulator-independent results and the role of two-pion exchange. Eur. Phys. J. A **36**, 315 (2008)
49. Machleidt R., Liu P., Entem D.R., Arriola E.R.: Renormalization of the leading-order chiral nucleon-nucleon interaction and bulk properties of nuclear matter. Phys. Rev. C **81**, 024001 (2010)
50. Valderrama M.P.: Perturbative Renormalizability of Chiral Two Pion Exchange in Nucleon-Nucleon Scattering. Phys. Rev. C **83**, 024003 (2011)
51. Valderrama M.P.: Perturbative Renormalizability of Chiral Two Pion Exchange in Nucleon-Nucleon Scattering: P- and D-waves. Phys. Rev. C **84**, 064002 (2011)
52. Timoteo, V., Frederico, T., Delfino, A., Tomio, L.: Nucleon-nucleon scattering within a multiple subtractive renormalization approach. Phys. Rev. C **83**, 064005 (2011)
53. Long, B., Yang, C.J.: Renormalizing chiral nuclear forces: Triplet channels. Phys. Rev. C **85**, 034002 (2012)
54. Birse, M.C.: The renormalization group and nuclear forces. arXiv:1109.2797 (2011)
55. Kaiser N.: Chiral 3π -exchange NN potentials: Results for representation-invariant classes of diagrams. Phys. Rev. C **61**, 014003 (2000);
56. Kaiser N.: Chiral 3π -exchange NN potentials: Results for diagrams proportional to g_A^4 and g_A^6 . Phys. Rev. C **62**, 024001 (2000)
57. Blankenbecler, R., Sugar, R.: Linear integral equations for relativistic multichannel scattering. Phys. Rev. **142**, 1051 (1966)
58. Stoks, V.G.J., Klomp, R.A.M., Rentmeester, M.C.M., de Swart, J.J.: Partial wave analysis of all nucleon-nucleon scattering data below 350-MeV. Phys. Rev. C **48**, 792 (1993)
59. Arndt, R.A., Strakovsky, I.I., Workman, R.L.: SAID, Scattering Analysis Interactive Dial-in computer facility, George Washington University (formerly Virginia Polytechnic Institute), solution SM99 (Summer 1999); for more information see, e. g., Arndt, R.A., Strakovsky, I.I., Workman, R.L.: An Updated analysis of N N elastic scattering data to 1.6-GeV. Phys. Rev. C **50**, 2731 (1994)
60. Epelbaum, E., Gegelia, J.: Regularization, renormalization and 'peratization' in effective field theory for two nucleons. Eur. Phys. J. **A41**, 341 (2009)
61. Lepage G.P.: How to Renormalize the Schrödinger Equation. arXiv:nucl-th/9706029